Molecular Syndromology

FAM222B Is Not a Likely Novel Candidate Gene for Cerebral Cavernous Malformations

Stefanie Spiegler[a]   Bettina Kirchmaier[b, f]   Matthias Rath[a]

G. Christoph Korenke[c]   Fabian Tetzlaff[d]   Maartje van de Vorst[g]

Kornelia Neveling[g]   Amparo Acker-Palmer[b]   Andreas W. Kuss[a]

Christian Gilissen[g]   Andreas Fischer[d]   Stefan Schulte-Merker[e, f]   Ute Felbor[a]

[a]Department of Human Genetics, University Medicine Greifswald and Interfaculty Institute of Genetics and Functional Genomics, University of Greifswald, Greifswald, [b]Institute of Cell Biology and Neuroscience and Buchmann Institute for Molecular Life Sciences (BMLS), University of Frankfurt, Frankfurt am Main, [c]Department of Neuropaediatrics, Children's Hospital, Oldenburg, [d]Vascular Signaling and Cancer, German Cancer Research Center (DKFZ), Heidelberg, and [e]Institute for Cardiovascular Organogenesis and Regeneration, Cells-in-Motion Cluster of Excellence, Faculty of Medicine, University of Münster, Münster, Germany; [f]Hubrecht Institute – KNAW & UMC Utrecht, Utrecht, and [g]Department of Human Genetics, Radboud University Medical Centre, Nijmegen, The Netherlands

Abstract

Cerebral cavernous malformations (CCMs) are prevalent slow-flow vascular lesions which harbour the risk to develop intracranial haemorrhages, focal neurological deficits, and epileptic seizures. Autosomal dominantly inherited CCMs were found to be associated with heterozygous inactivating mutations in 3 genes, *CCM1 (KRIT1)*, *CCM2 (MGC4607)*, and *CCM3 (PDCD10)* in 1999, 2003 and 2005, respectively. Despite the availability of high-throughput sequencing techniques, no further *CCM* gene has been published since. Here, we report on the identification of an autosomal dominantly inherited frameshift mutation in a gene of thus far unknown function, *FAM222B (C17orf63)*, through exome sequencing of CCM patients mutation-negative for *CCM1-3*. A yeast 2-hybrid screen revealed interactions of FAM222B with the tubulin cytoskeleton and STAMBP which is known to be associated with microcephaly-capillary malformation syndrome. However, a phenotype similar to existing models was not found, neither in *fam222bb/fam222ba* double mutant zebrafish generated by transcription activator-like effector nucleases nor in an in vitro sprouting assay using human umbilical vein endothelial cells transfected with siRNA against *FAM222B*. These observations led to the assumption that aberrant *FAM222B* is not involved in the formation of CCMs.

© 2016 S. Karger AG, Basel

Cerebral cavernous malformations (CCMs) are angiographically occult vascular malformations of the central nervous system. With the availability of high-resolution

Prof. Dr. U. Felbor, MD
Department of Human Genetics, University Medicine Greifswald
Fleischmannstrasse 42–44
DE–17475 Greifswald (Germany)
E-Mail felbor@uni-greifswald.de

magnetic resonance imaging (MRI) including gradient-echo (GRE/T2*) and susceptibility-weighted imaging sequences, their prevalence has been demonstrated to be about 1:650 among neurologically asymptomatic people [Morris et al., 2009]. Familial CCM (MIM 116860, 603284, 603285) has been assumed to occur in close to 20% of all cases and is associated with the development of multiple CCMs earlier in life [Fischer et al., 2013]. At-risk family members are threatened by the uncertainties of recurrent haemorrhages which may cause chronic headache, epilepsy, neurological deficits, and haemorrhagic stroke with intrafamilial variability [Fauth et al., 2015].

Disease penetrance has been reported to be 63, 55, and 68% for individuals carrying a heterozygous loss-of-function (LOF) mutation in *CCM1*, *CCM2* or *CCM3*, respectively [Denier et al., 2006]. Fulminant disease courses with hemiparesis during the first years of life have only rarely been reported for *CCM1* and *CCM3* mutation carriers. However, one third of index patients were children or adolescents when referred for genetic testing [Spiegler et al., 2014]. The identification of a mutation within one of the known *CCM* genes in an index case enables predictive genetic testing of further at-risk family members. Most importantly, exclusion of a specific familial mutation relieves relatives and their families from unnecessary anxieties and medical examinations [Schröder et al., 2014].

If genetic screening of index cases follows stringent inclusion criteria, mutation detection rates are 87% for affected individuals with a positive family history and 57% for isolated cases carrying multiple CCMs, the overall proportions being 60% for *CCM1*, 18% for *CCM2*, and 22% for *CCM3* mutations [Spiegler et al., 2014]. While some of the isolated mutation-negative cases may be explained by the occurrence of postzygotic somatic mutations, mutation negativity for the known *CCM1–3* genes in familial cases alludes to further genetic heterogeneity. In this study, we analysed *FAM222B* as a putative candidate gene for CCMs and showed that it does not play a role in maintaining vascular integrity in vitro and in vivo.

Materials and Methods

Clinical Samples

After step-wise sequencing, MLPA and transcript analyses of *CCM1–3* had been performed with informed consent according to the German Gene Diagnostics Act for all index cases fulfilling the established criteria [Stahl et al., 2008; Spiegler et al., 2014]. For the 4 isolated cases and the father-daughter duo (fig. 1A), multiple cavernomas have been verified by MRI. Genomic DNA was isolated from peripheral blood leukocytes using standard protocols.

Whole Exome Sequencing

For exome capture, the SOLiD-optimized SureSelect Human All Exon 50Mb kit (Agilent Technologies, Santa Clara, Calif., USA) was used following the manufacturer's instructions. Sequencing on a SOLiD 5500XL platform (Life Technologies – Thermo Fisher, Waltham, Mass., USA) was performed in pools of 4 samples on 2 lanes of a sequencing slide. On average, mean target sequencing depth was 29 and 67% of the exome was covered at least 10 times. To verify the results and increase the depth of coverage, target enrichment and exome sequencing was repeated for all 4 isolated probands and the father-daughter duo (mean target sequencing depth was 78×). In brief, primary data analysis and variant annotation was done with the bioinformatics pipeline from Radboud University Nijmegen Medical Centre (Nijmegen, The Netherlands) as described [Neveling et al., 2013]. Using an overlap strategy for index probands I, III–VI (fig. 1A) [Hoischen et al., 2010, 2011], we searched for heterozygous mutations that occur in a single gene in at least 2 patients and are expected to disrupt protein function (frameshift, stop, and splice mutations). For the father-daughter duo (probands I and II, fig. 1A), a linkage strategy based on the suspected autosomal dominant mode of inheritance was applied. For both approaches, exclusion of frequent variants in an in-house database consisting of 670 exomes as well as frequent variants in dbSNP132 (>1%), the exome variant server (EVS, >1%) and gonosomes was followed by manual validation of the remaining genes through evaluation of mapped reads, conservation scores, expression data, and known phenotypes in mice or zebrafish. Following validation of the *FAM222B* (ENSEMBL ENST00000581407, GenBank NM_018182) frameshift mutation, verification analyses were done in a cohort of 15 further CCM probands that presented with multiple cavernomas on MRI but without a causative mutation in *CCM1–3*. Sanger sequencing was performed on an ABI 3130xl automated sequencer (Applied Biosystems – Thermo Fisher) using the BigDye Terminator Cycle Sequencing v3.1 kit (Applied Biosystems – Thermo Fisher). *FAM222B* primer sequences are available on request.

Yeast 2-Hybrid Analysis

The screen was carried out by Hybrigenics Services SAS, Paris, France (http://www.hybrigenics-services.com). To screen a human fetal brain cDNA library, the cDNA coding for full-length human *FAM222B* (SC320887, Origene, Rockville, Md., USA) was cloned as a C-terminal fusion to the DNA-binding domain of LexA into the pB27 vector (N-LexA-FAM222B-C). Yeast cells were transfected and 90 million clones (9× coverage of the library complexity) were screened, providing a total of 197 positive clones on selective medium supplemented with 1 mM 3-aminotriazole. Positive clones were sequenced at 5′- and 3′-junctions and the identification of corresponding interacting proteins in the GenBank database was performed on a fully automated basis. Interactions were attributed by a confidence score as described [Formstecher et al., 2005].

In vivo Studies

Zebrafish were maintained in accordance with the approved institutional protocols at the Hubrecht Institute. For the generation of a *fam222bb* and *fam222ba* mutant zebrafish line, transcription activator-like effector nuclease (TALEN)-mediated genome editing was performed as described elsewhere [van Impel et al., 2014]. TALEN sequences were identified in candidate genes using

Fig. 1. A Probands that were analysed by whole exome sequencing. The daughter (I) experienced complex focal epilepsy, whereas her father (II) presented with headaches, focal epilepsy, and right-sided hemiparesis. The boy (III) reported recurrent headaches. Brain MRI of his parents did not show any lesions. The girl (IV) presented with acute strabismus, facial nerve paralysis and headaches. Proband V presented with severe psychomotor retardation and paraplegia during early childhood. Proband VI has multiple cerebral and spinal CCMs resulting in paraplegia after intramedullary bleeding. The age of onset is given next to the probands in years. Axial (**B–D**) and coronal (**E**) MRI of proband I. T2- (**B**), FLAIR- (**C**), (GRE) T2*- (**D**), and T1-weighted (**E**) gadolinium-enhanced MRI of patient I who presented with seizures at 5 years of age. Arrowheads indicate the cavernous lesion. Wild-type (**F**) and mutant (**G**) sequences of the variant in *FAM222B* identified during WES in affected probands I and II.
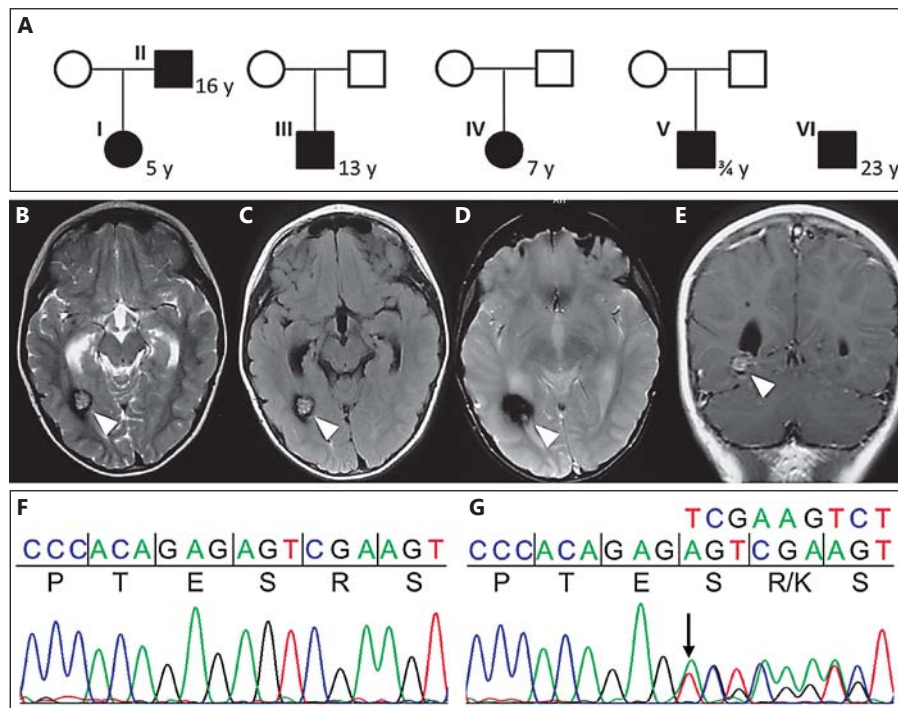
TAL Effector Nucleotide Targeter 2.0 (https://tale-nt.cac.cornell.edu/). TALEN binding sites in *fam222bb* exon 3 were: TAL1 5′-TACCCACCTCAGGTCA-3′, TAL2 5′-TCTTGGCCATAGT-CAAA-3′. For *Fam222ba* the TALEN recognition sites were placed in exon 2: TAL1 5′-TGTTTCTACCTCAACCATTCC-3′, TAL2 5′-GGGCTCCATCAGGGCCGGCA-3′. Lines were outcrossed into a *Tg(kdrl:GFP)^{s843}/Tg(gata1:dsRed)^{sd2}* background.

Image Acquisition

For all imaging experiments, larvae were treated with 0.2 mM 1-phenyl-2-thiocarbamide no later than 24 h after fertilization to prevent the formation of pigment in skin cells. Confocal imaging was performed on living embryos embedded in 0.8–1% low melting point agarose (Invitrogen – Thermo Fisher) with tricaine. Imaging of the vascular network was achieved using Leica SPE and SP7 microscopes. Images were visualized by ImageJ FIJI software (http://fiji.sc/Fiji) or Leica LAS AF software and processed with Adobe Photoshop CS5.1.

In vitro Studies

Primary human umbilical vein endothelial cells (HUVECs) were transfected with small interfering RNA (siRNA s226861, Ambion – Thermo Fisher) (final concentration: 10 nM) and 8 µl of oligofectamine (Invitrogen – Thermo Fisher) according to the manufacturer's protocol. OPTI-MEM was replaced after 4 h by ECGM (PromoCell, Heidelberg, Germany) containing 10% FCS. Total RNA was extracted using PeqGold (Peqlab – VWR, Radnor, Pa., USA) reagent and purified using Absolutely RNA Miniprep Kit (Agilent Technologies). Reverse transcription was done with First Strand cDNA Synthesis Kit (Thermo Fisher) and knockdown was assessed using the QuantStudio 3D Digital PCR System

(LifeTechnologies – Thermo Fisher) or the LightCycler480 instrument (Roche, Rotkreuz, Swiss) with a specific Universal Probe Library Assay for *FAM222B* (Roche, UPL #38, primer left: 5′-CCAGAACAGCTTGATGCAAA-3′, primer right: 5′-CATG-GCCAGGCTCTGTTC-3′). For spheroid formation, the cells were harvested one day after transfection and cultured as hanging drops for another 24 h. After crop of the spheroids, they were embedded into a collagen matrix. Following polymerisation, they were stimulated with basal medium or a medium containing 25 ng/ml VEGF or FGF2 growth factors. After 24 h, sprouting was terminated by adding 10% paraformaldehyde to the wells.

Results

Identification of a Frameshift Mutation in FAM222B through Exome Analysis

To address the question of further genetic heterogeneity for CCMs, exome sequencing was performed for one familial (father and daughter) and 4 isolated cases (fig. 1A) that had remained mutation-negative for *CCM1–3* [Stahl et al., 2008]. Of note, all probands reported early disease onset with a mean age at manifestation of 10.8 years (ranging from 9 months to 23 years). Clinical symptoms varied but tended to be severe with refractory epilepsy (individual I) and significant neurological deficits because of recurrent bleedings (individual II, IV–VI).
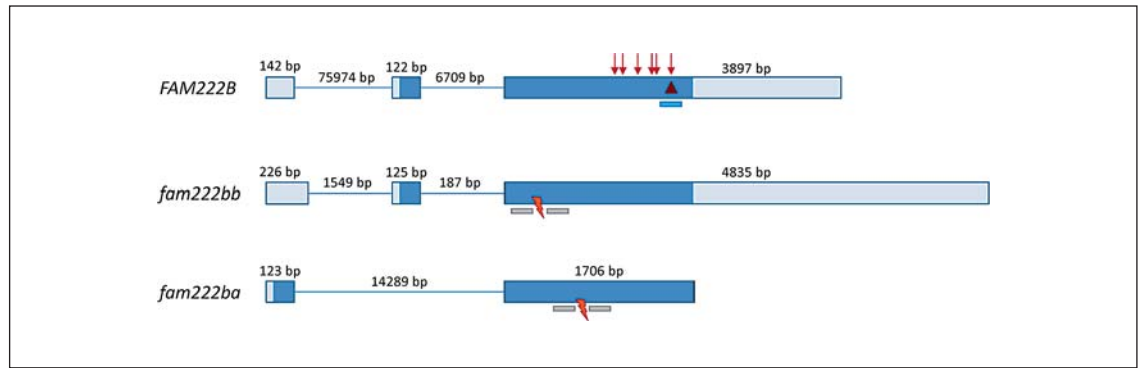
Fig. 2. Genomic organisation of human *FAM222B* and zebrafish orthologues *fam222bb* and *fam222ba*. Exons are shown as boxes, introns as thin lines, lengths are given in bp. Coding parts are highlighted in dark blue, non-coding in light blue. ENSEMBL transcripts are ENST00000581407 for human *FAM222B*, ENSDART00000154504 for zebrafish *fam222bb*, and ENSDART00000145247 for zebrafish *fam222ba*. The 2-bp deletion identified in probands I and II is delineated by a red triangle. Listed LOF mutations from the ExAC browser are represented by red arrows. The binding site of the siRNA used for in vitro knockdown of *FAM222B* is highlighted as a blue bar. Binding sites of TALE nucleases are shown as grey bars and the red flashes indicate the region where the mutagenesis took place.

Whole exome sequencing of DNA from these patients led to ~210,000 variants in total. Bioinformatic filtering following the overlap strategy [Gilissen et al., 2012] resulted in only 1 compelling candidate gene, *FAM222B* (*C17orf63*), harbouring a Sanger-validated 2-bp deletion, c.1651_1652delAG (p.Arg552Lysfs*10), which segregated with CCMs within the family (fig. 1A, individuals I and II), but was not observed in any of the other 4 isolated cases. The second exome analyses with higher coverage again revealed the known *FAM222B* frameshift mutation as the only compelling candidate.

Among the 6,503 controls from the NHLBI GO Exome Sequencing Project (EVS, Version v.0.0.14; http://evs.gs.washington.edu/EVS/), no LOF mutation was found in *FAM222B* which consists of 1 non-coding and 2 coding exons with the ATG initiator codon located in the second exon (fig. 2). Sanger sequencing of the entire coding region and adjacent splice sites of *FAM222B* was performed for 15 further *CCM1–3* mutation-negative probands [Spiegler et al., 2014]. However, this did not reveal a second CCM individual carrying a *FAM222B* LOF or likely pathogenic missense mutation. Since the additional CCM individuals tested were mainly isolated cases with disease onset later in life (ranging from 12 to 59 years), the lacking genetic verification of *FAM222B* may not only be due to genetic heterogeneity, but also to phenocopies or somatic mosaicism [McDonald et al., 2014; Lodato et al., 2015].

Yeast 2-Hybrid Interactors of FAM222B Are Components of the Cytoskeleton and the RAS-MAPK and PI3K/AKT/mTOR Pathways

FAM222B encodes for a widely expressed 60 kDa protein of thus far unknown function (Multi-Omics Profiling Expression Database, PaxDb, The Human Protein Atlas). In silico analyses indicated the absence of a signal peptide, transmembrane domain or membrane anchor. In order to get a first idea on its putative roles, a human fetal brain cDNA library was screened using full-length human FAM222B as a bait in a LexA-based yeast 2-hybrid system. The most confident binding partners of FAM222B are listed in online supplementary table 1 (see www.karger.com/doi/10.1159/000446884, for all online suppl. material) and can be grouped into cytoskeletal components and proteins that are involved in different signalling cascades. In particular, the putative interactions of FAM222B with the tubulin cytoskeleton (TUBB, TUBB2A, TUBB2B, and TUBA1B) represented a possible link to subcellular localisation and function of known CCM proteins. Of note, CCM1 has been suggested to be a microtubule-associated protein [Gunel et al., 2002; Béraud-Dufour et al., 2007; Fisher and Boggon, 2014]. Another interactor of FAM222B, *STAM*-binding protein (STAMBP), has been described as a microtubule-associated protein involved in endosomal sorting of ubiquitinated proteins [Tsang et al., 2006; McDonell et al., 2013]. Mutations in *STAMBP* are associated with microcephaly-capillary malformation syndrome and also cause dysreg-

Fig. 3. *fam222bb* and *fam222ba* double mutants display no CCM-specific vascular phenotype. **A** Schematic of Fam222bb and Fam222ba domain structure, indicating the position of *fam222bb^hu10539* and *fam222ba^hu10755* amino acid frameshifts and premature stop mutations (red bars). FAM222A: domain of unknown function. Examples of sequencing reads of *fam222bb* (**B**) and *fam222ba* (**C**) wild-type, heterozygous and homozygous zebrafish embryos; the respective 10-bp deletion is marked in the wild-type read. **D** Brightfield picture and confocal micrograph of 3 dpf *fam222bb/fam222ba* double mutant zebrafish trunk bearing Tg*(kdrl:egfp)^s843* (green).
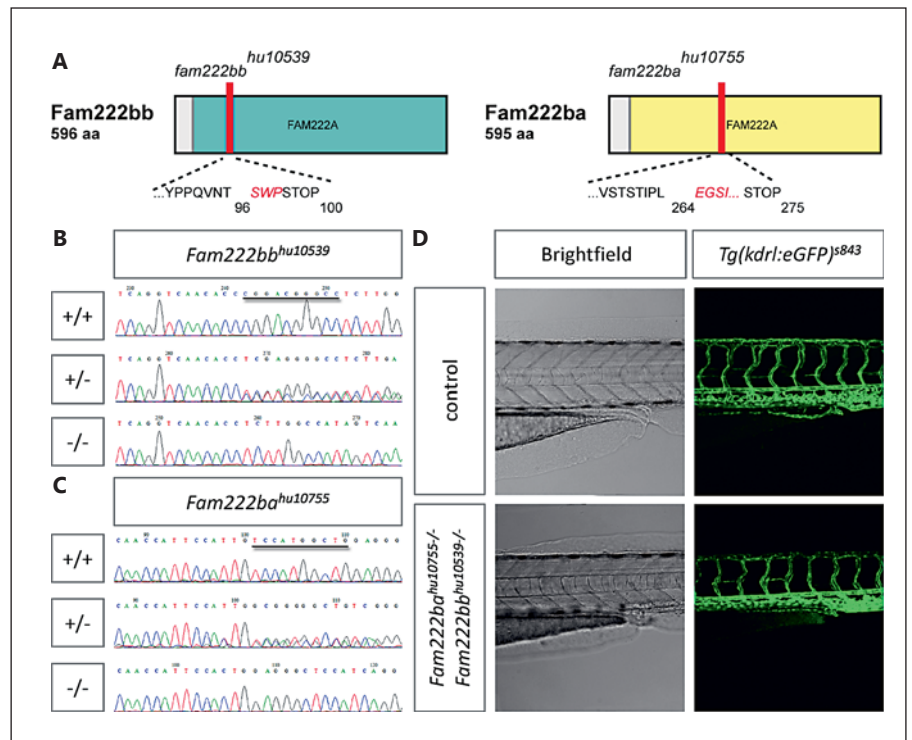
ulation of the RAS-MAPK and PI3K/AKT/mTOR pathways [McDonell et al., 2013]. This suggested that FAM222B may act in concert with the known CCM proteins in common networks.

TALEN-Generated fam222bb/fam222ba Double Mutants Display Normal Vascular Morphology

Large-scale forward genetic screens have identified a characteristic cardiovascular phenotype in zebrafish carrying mutations in either *ccm1* (*santa*) or *ccm2* (*valentine*) [Chen et al., 1996; Stainier et al., 1996; Mably et al., 2006; Hogan et al., 2008]. At 2–4 days after fertilisation, this phenotype mainly consists of dilated, slowly contracting heart chambers, disturbed blood circulation and pericardial edema, disorganised sprouting of subintestinal vessels, and an enlarged caudal vein which is spatially barely distinguishable from the caudal artery. All these features could later be reproduced by simultaneous knockdown of *ccm3a* and its duplicate *ccm3b* using antisense morpholino oligomers [Voss et al., 2009]. However, since these oligomers are known to often have off-target effects [Kok et al., 2015], we intended to analyse the effects of a *fam222b* knockout in mutant zebrafish embryos generated by TALENs (fig. 2). First, a founder fish bearing a 10-bp deletion was selected since this frameshift

mutation in the *fam222bb* gene (*fam222bb^hu10539*) is expected to result in protein truncation or nonsense-mediated decay. Then, the founder fish was crossed with Tg*(kdrl:GFP)^s843*/Tg*(gata1:dsRed)^sd2* transgenic zebrafish in order to be able to visualise vascular morphology. Homozygous mutant, heterozygous and wild-type progeny was detected at the expected ratios, but no overt phenotype could be seen in embryos until 5 days after fertilisation.

In 2013, a new update of the zebrafish reference genome assembly (Zv9) revealed the existence of a *fam222bb* duplicate, *fam222ba*. Thus, a double mutant line was generated carrying a 10-bp deletion in the *fam222ba* gene (*fam222ba^hu10755*) in addition to the above-mentioned *fam222bb^hu10539* mutation. However, homozygous double mutants, 7 out of 59 analysed, were again indistinguishable from wild-type siblings 5 days after fertilisation (fig. 3). In addition, homozygous double mutants were viable to adulthood.

Normal Sprouting of HUVECs after siRNA-Mediated Knockdown of FAM222B

Silencing of either *CCM1* or *CCM3* had been shown to induce sprouting angiogenesis in vitro [Wüstehube et al., 2010; Schleider et al., 2011; You et al., 2013]. Therefore, a

Table 1. Absolute numbers of LOF mutations in the known *CCM* and *FAM222B* genes as listed in the ExAC browser

Gene	Nonsense	Frameshift	Splice	Total	HGMD	Overlapping	EVS
CCM1	6	7 (6)	3	15 (14)	6	2 (1× fs, 1× nonsense)	2
CCM2	1	0	2	3	1	2 (splice site)	0
CCM3	0	0	0	0	0	0	0
FAM222B	5 (2)	8 (5)	0	13 (7)	–	–	0

The number of unique LOF mutations is given in brackets. The column HGMD indicates the number of mutations listed as disease causing in the HGMD database, another mutation at the same position is classified as overlapping (source: HGMD® Professional database 2015.4). The column EVS specifies the number of LOF mutations included in the Exome Variant Database (http://evs.gs.washington.edu/EVS/). None of them are listed in the HGMD database. fs = Frameshift.

specific siRNA was used to knock down *FAM222B* (fig. 2) in HUVECs and to study the corresponding in vitro angiogenic phenotype in a 3D, spheroid-based sprouting assay as previously described [Korff and Augustin, 1998; Heiss et al., 2015]. Although *FAM222B* expression of siRNA-treated HUVECs was efficiently downregulated, no activation of angiogenic sprouting could be observed (fig. 4). Neither length nor number of sprouts were significantly altered in *FAM222B* knockdown spheroids upon stimulation with VEGF or FGF2. These observations were in line with the lack of a vascular phenotype in *fam222bb* [hu10539]/*fam222ba* [hu10755] double mutant zebrafish and strengthened the assumption that *FAM222B* is not involved in pathways keeping endothelial cells quiescent.

Discussion

The identification of inactivating mutations in *CCM1*, *CCM2*, and *CCM3* in individuals affected with CCM led to the insight that the 3 gene products contribute to regulate angiogenesis and to maintain vascular homeostasis. Similarly, the association of a *FAM222B* frameshift mutation with early disease manifestation in an affected daughter and her father had raised the hope that this gene of thus far unknown function might be essential for vascular morphogenesis and integrity. However, despite the recent observation that deleterious mutations may activate compensatory networks in zebrafish [Rossi et al., 2015], our experimental studies using in vitro and in vivo angiogenesis model systems suggest that FAM222B is not required for vasculogenesis and angiogenesis.

During the course of our experiments, the Exome Aggregation Consortium (ExAC) database was published, which comprises 60,706 exomes from individuals not af-
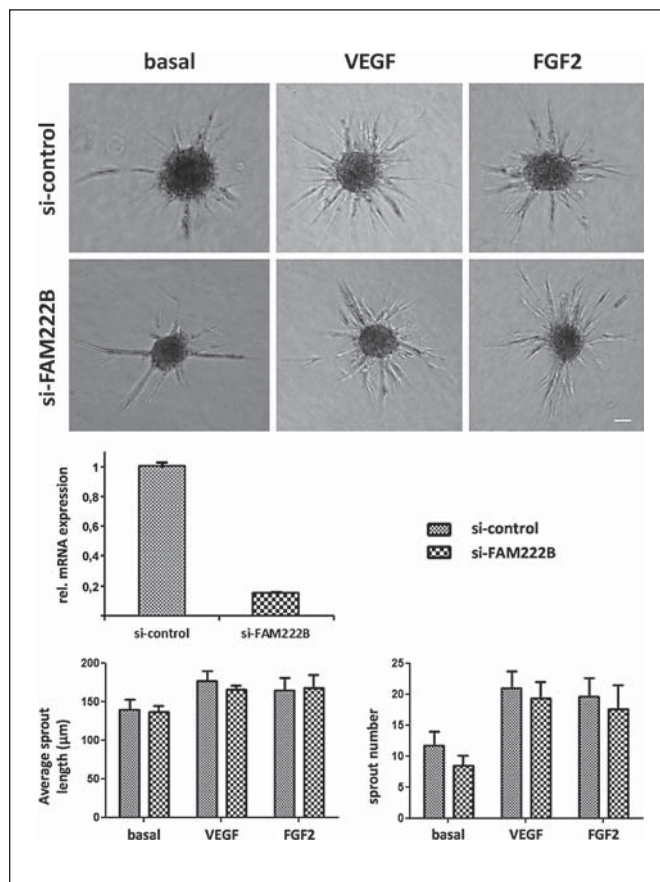

Fig. 4. Spheroid sprouting of HUVECs transfected with negative control siRNA and siRNA against *FAM222B*. Top row: after transfection, HUVEC spheroids were embedded in a collagen matrix under basal condition and with addition of 25 ng/ml VEGF or FGF2 growth factors. Middle row: transfection of HUVEC with siRNA against *FAM222B* led to ~85% mRNA knockdown rates compared to non-silencing control siRNA. Bottom: average sprout length and number of sprouts per spheroid are not significantly altered between control conditions and *FAM222B* knockdown. n = 4 experiments. Scale bar = 50 μm. Bar graphs depict mean values, error bars show standard error of the mean.

fected by severe paediatric diseases. While no *FAM222B* LOF mutation was found in 6,503 controls from the EVS at the time the exome analyses had been performed, 13 heterozygous *FAM222B* LOF mutations were later found in the ExAC database. The 2-bp deletion c.1651_1652delAG which segregated with CCM in the familial case is listed 3 times in ExAC (Cambridge, Mass., Version 0.3/ 02/2016, http://exac.broadinstitute.org/) (table 1).

Therefore, we reviewed the ExAC database for LOF mutations in the known *CCM1–3* genes (table 1): it is remarkable that 6 of the 15 LOF mutations within *CCM1* and 1 of 3 LOF mutations within *CCM2* have been described as disease causing in the HGMD database (HGMD® Professional database 2015.4; online suppl. table 2). This fact may be reconciled with the observation that disease penetrance is age-dependent and incomplete and disease manifestation variable for CCM. Notably, asymptomatic carrier parents harbouring at least one CCM have been observed in 75% of 'apparently sporadic index cases with multiple lesions' [Labauge et al., 1998], while bona fide de novo mutations have only rarely been documented for *CCM1* [Stahl et al., 2008] and *CCM3* [Bergametti et al., 2005]. In contrast to *CCM1* and *CCM2*, not a single LOF mutation within *CCM3* is mentioned in the ExAC database. This may be in line with the observation that 50–53% of index cases carrying a *CCM3* mutation became symptomatic prior to age 15 – mostly with early-onset cerebral haemorrhages [Denier et al., 2006; Spiegler et al., 2014; Shenkar et al., 2015].

For the exome study presented here, we selected affected individuals with early and rather severe disease onset in order to search for a putative fourth causative gene in the remaining 13–43% of *CCM1–3* mutation-negative probands. Thus, a bioinformatic filtering process considering the ExAC data may orientate towards the *CCM2* and *CCM3* data in ExAC and rather not allow more than 3 LOF mutations within the same gene and no recurrence for exactly the same mutation. On the one hand, our experimental data seem to support such strict filter criteria. On the other hand, *CCM1* would have been excluded. Therefore, filter criteria need to be individually adapted even within one genetically heterogeneous condition [Albers et al., 2012], and a small number of occurrences in ExAC may not disqualify a candidate gene.

The advent of the ExAC database also prompted us to review disease prevalence of *CCM1–3* LOF mutations. Based on the ExAC data, 1 in 3,373 individuals that do not display a severe paediatric disease harbour an inactivating heterozygous *CCM1* or *CCM2* germline mutation.

Given that almost all *CCM* mutation carriers reveal at least one cavernous lesion if high-resolution MRI is performed [Denier et al., 2006], one can assume that the carriers of the 18 LOF *CCM1–2* mutations listed in the ExAC database (table 1) bear asymptomatic CCMs that would have been detected in high-resolution MRI or autopsy study series. These had revealed that CCM occurs with a prevalence of about 0.5%/1:185–1:255 in hospital-based series [Del Curling et al., 1991; Robinson et al., 1991] and autopsies [Otten et al., 1989]. For neurologically asymptomatic people, the prevalence is lower and has been reported to be about 0.15%/1:676 [Morris et al., 2009] in a large meta-analysis. A recent prospective, population-based cohort study also pointed out that 24 of 139 (i.e., 17%) adults with CCMs had multiple lesions [Al-Shahi Salman et al., 2012]. In conclusion, the ExAC data most likely reflect the frequency of asymptomatic familial cases carrying *CCM1* and *CCM2* mutations and are in agreement with the previously published assumption that close to 20% of Caucasians that carry at least one CCM are in fact familial [Denier et al., 2006; Fischer et al., 2013].

Conclusion

Taken together, our experimental results as well as the ExAC data, *FAM222B* variants would currently not qualify to be used for predictive genetic testing of relatives. Even with high-throughput sequencing techniques, it remains challenging to identify unambiguously disease-causing mutations in a novel gene for a genetically heterogeneous condition with incomplete penetrance and variable clinical manifestations such as CCM. A further major obstacle is the likely occurrence of somatic mutations in a proportion of isolated CCM cases with multiple lesions but *CCM1–3* mutation negativity in lymphocytes.

Statement of Ethics

Written informed consent for exome analyses was obtained from all study participants in accordance with the ethical guidelines of the Declaration of Helsinki and approval of the local ethics committee of the University Medicine Greifswald (registration No.: BB 067/13).

Disclosure Statement

The authors declare no conflicts of interest.

References

Albers CA, Paul DS, Schulze H, Freson K, Stephens JC, et al: Compound inheritance of a low-frequency regulatory SNP and a rare null mutation in exon-junction complex subunit RBM8A causes TAR syndrome. Nat Genet 44: 435–439 (2012).

Al-Shahi Salman R, Hall JM, Horne MA, Moultrie F, Josephson CB, et al: Untreated clinical course of cerebral cavernous malformations: a prospective, population-based cohort study. Lancet Neurol 11:217–224 (2012).

Béraud-Dufour S, Gautier R, Albiges-Rizo C, Chardin P, Faurobert E: Krit1 interactions with microtubules and membranes are regulated by Rap1 and integrin cytoplasmic domain associated protein-1. FEBS J 274:5518–5532 (2007).

Bergametti F, Denier C, Labauge P, Arnoult M, Boetto S, et al: Mutations within the programmed cell death 10 gene cause cerebral cavernous malformations. Am J Hum Genet 76:42–51 (2005).

Chen JN, Haffter P, Odenthal J, Vogelsang E, Brand M, et al: Mutations affecting the cardiovascular system and other internal organs in zebrafish. Development 123:293–302 (1996).

Del Curling O Jr, Kelly DL Jr, Elster AD, Craven TE: An analysis of the natural history of cavernous angiomas. J Neurosurg 75:702–708 (1991).

Denier C, Labauge P, Bergametti F, Marchelli F, Riant F, et al: Genotype-phenotype correlations in cerebral cavernous malformations patients. Ann Neurol 60:550–556 (2006).

Fauth C, Rostasy K, Rath M, Gizewski E, Lederer AG, et al: Highly variable intrafamilial manifestations of a CCM3 mutation ranging from acute childhood cerebral haemorrhage to late-onset meningiomas. Clin Neurol Neurosurg 128:41–43 (2015).

Fischer A, Zalvide J, Faurobert E, Albiges-Rizo C, Tournier-Lasserve E: Cerebral cavernous malformations: from CCM genes to endothelial cell homeostasis. Trends Mol Med 19: 302–308 (2013).

Fisher OS, Boggon TJ: Signaling pathways and the cerebral cavernous malformations proteins: lessons from structural biology. Cell Mol Life Sci 71:1881–1892 (2014).

Formstecher E, Aresta S, Collura V, Hamburger A, Meil A, et al: Protein interaction mapping: a Drosophila case study. Genome Res 15:376–384 (2005).

Gilissen C, Hoischen A, Brunner HG, Veltman JA: Disease gene identification strategies for exome sequencing. Eur J Hum Genet 20:490–497 (2012).

Gunel M, Laurans MS, Shin D, DiLuna ML, Voorhees J, et al: KRIT1, a gene mutated in cerebral cavernous malformation, encodes a microtubule-associated protein. Proc Natl Acad Sci USA 99:10677–10682 (2002).

Heiss M, Hellström M, Kalén M, May T, Weber H, et al: Endothelial cell spheroids as a versatile tool to study angiogenesis in vitro. FASEB J 29:3076–3084 (2015).

Hogan BM, Bussmann J, Wolburg H, Schulte-Merker S: ccm1 cell autonomously regulates endothelial cellular morphogenesis and vascular tubulogenesis in zebrafish. Hum Mol Genet 17:2424–2432 (2008).

Hoischen A, van Bon BW, Gilissen C, Arts P, van Lier B, et al: De novo mutations of SETBP1 cause Schinzel-Giedion syndrome. Nat Genet 42:483–485 (2010).

Hoischen A, van Bon BW, Rodríguez-Santiago B, Gilissen C, Vissers LE, et al: De novo nonsense mutations in ASXL1 cause Bohring-Opitz syndrome. Nat Genet 43:729–731 (2011).

Kok FO, Shin M, Ni CW, Gupta A, Grosse AS, et al: Reverse genetic screening reveals poor correlation between morpholino-induced and mutant phenotypes in zebrafish. Dev Cell 32: 97–108 (2015).

Korff T, Augustin HG: Integration of endothelial cells in multicellular spheroids prevents apoptosis and induces differentiation. J Cell Biol 143:1341–1352 (1998).

Labauge P, Laberge S, Brunereau L, Levy C, Tournier-Lasserve E, et al: Hereditary cerebral cavernous angiomas: clinical and genetic features in 57 French families. Société Française de Neurochirurgie. Lancet 352:1892–1897 (1998).

Lodato MA, Woodworth MB, Lee S, Evrony GD, Mehta BK, et al: Somatic mutation in single human neurons tracks developmental and transcriptional history. Science 350:94–98 (2015).

Mably JD, Chuang LP, Serluca FC, Mohideen MA, Chen JN, Fishmann MC: santa and valentine pattern concentric growth of cardiac myocardium in the zebrafish. Development 133:3139–3146 (2006).

McDonald DA, Shi C, Shenkar R, Gallione CJ, Akers AL, et al: Lesions from patients with sporadic cerebral cavernous malformations harbor somatic mutations in the CCM genes: evidence for a common biochemical pathway for CCM pathogenesis. Hum Mol Genet 23: 4357–4370 (2014).

McDonell LM, Mirzaa GM, Alcantara D, Schwartzentruber J, Carter MT, et al: Mutations in STAMBP, encoding a deubiquitinating enzyme, cause microcephaly-capillary malformation syndrome. Nat Genet 45:556–562 (2013).

Morris Z, Whiteley WN, Longstreth WT Jr, Weber F, Lee YC, et al: Incidental findings on brain magnetic resonance imaging: systematic review and meta-analysis. BMJ 339:b3016 (2009).

Neveling K, Martinez-Carrera LA, Hölker I, Heister A, Verrips A, et al: Mutations in BICD2, which encodes a golgin and important motor adaptor, cause congenital autosomal-dominant spinal muscular atrophy. Am J Hum Genet 92:946–954 (2013).

Otten P, Pizzolato GP, Rilliet B, Berney J: 131 cases of cavernous angioma (cavernomas) of the CNS, discovered by retrospective analysis of 24, 535 autopsies (in French). Neurochirurgie 35:82–83 (1989).

Robinson JR, Awad IA, Little JR: Natural history of the cavernous angioma. J Neurosurg 75: 709–714 (1991).

Rossi A, Kontarakis Z, Gerri C, Nolte H, Hölper S, et al: Genetic compensation induced by deleterious mutations but not gene knockdowns. Nature 524:230–233 (2015).

Schleider E, Stahl S, Wüstehube J, Walter U, Fischer A, Felbor U: Evidence for anti-angiogenic and pro-survival functions of the cerebral cavernous malformation protein 3. Neurogenetics 12:83–86 (2011).

Schröder W, Najm J, Spiegler S, Mair M, Viera J, et al: Predictive genetic testing of at-risk relatives requires analysis of all CCM genes after identification of an unclassified CCM1 variant in an individual affected with cerebral cavernous malformations. Neurosurg Rev 37: 161–165 (2014).

Shenkar R, Shi C, Rebeiz T, Stockton RA, McDonald DA, et al: Exceptional aggressiveness of cerebral cavernous malformation disease associated with *PDCD10* mutations. Genet Med 17:188–196 (2015).

Spiegler S, Najm J, Liu J, Gkalympoudis S, Schröder W, et al: High mutation detection rates in cerebral cavernous malformation upon stringent inclusion criteria: one-third of probands are minors. Mol Genet Genomic Med 2:176–185 (2014).

Stahl S, Gaetzner S, Voss K, Brackertz B, Schleider E, et al: Novel *CCM1*, *CCM2*, and *CCM3* mutations in patients with cerebral cavernous malformations: in-frame deletion in *CCM2* prevents formation of a CCM1/CCM2/CCM3 protein complex. Hum Mutat 29:709–717 (2008).

Stainier DY, Fouquet B, Chen JN, Warren KS, Weinstein BM, et al: Mutations affecting the formation and function of the cardiovascular system in the zebrafish embryo. Development 123:285–292 (1996).

Tsang HT, Connell JW, Brown SE, Thompson A, Reid E, Sanderson CM: A systematic analysis of human CHMP protein interactions: additional MIT domain-containing proteins bind to multiple components of the human ESCRT III complex. Genomics 88:333–346 (2006).

van Impel A, Zhao Z, Hermkens DM, Roukens MG, Fischer JC, et al: Divergence of zebrafish and mouse lymphatic cell fate specification pathways. Development 141:1228–1238 (2014).

Voss K, Stahl S, Hogan BM, Reinders J, Schleider E, et al: Functional analyses of human and zebrafish 18-amino acid in-frame deletion pave the way for domain mapping of the cerebral cavernous malformation 3 protein. Hum Mutat 30:1003–1011 (2009).

Wüstehube J, Bartol A, Liebler SS, Brütsch R, Zhu Y, et al: Cerebral cavernous malformation protein CCM1 inhibits sprouting angiogenesis by activating DELTA-NOTCH signaling. Proc Natl Acad Sci USA 107:12640–12645 (2010).

You C, Sandalcioglu IE, Dammann P, Felbor U, Sure U, Zuh Y: Loss of CCM3 impairs DLL4-Notch signalling: implication in endothelial angiogenesis and in inherited cerebral cavernous malformations. J Cell Mol Med 17:407–418 (2013).